Calculation of strain distributions at the edge of strained-layer structures

1990 J. Phys.: Condens. Matter 2 10289

(http://iopscience.iop.org/0953-8984/2/51/005)

J. Phys.: Condens. Matter **2** (1990) 10289–10302. Printed in the UK

Calculation of strain distributions at the edge of strained-layer structures

D A Faux† and J Haigh‡

† Physics Department, University of Surrey, Guildford GU2 5XH, UK

‡ British Telecom Research Laboratories, Martlesham Heath, Ipswich IP5 7RE, UK

Received 27 June 1990

Abstract. A method for calculating stress/strain distributions in structures containing one or more strained layers is presented. The theory, which is based on that presented by Treacy *et al*, is applied to the mesa laser structure containing either a single 3.5 nm strained layer or four evenly spaced 3.5 nm strained layers of $In_{0.7}Ga_{0.3}As$ grown on InGaAsP (lattice matched to InP). The theory includes the anisotropy of elastic constants in full. Cases of structures containing four strained layers are examined where the separation between the centre of the layers is 7.0 nm, 10.0 nm and 16.5 nm. The maximum shear strain in the case of the single layer is found to occur at the layer/barrier interface, close to the edge of the sample. This is, therefore, the region where dislocations are likely to nucleate. The shear strain is about 1.3% for the mesa structure which has a mismatch of 0.009. The presence of four closely spaced strained layers does not significantly affect the magnitude of the shear strain in the region of its maximum. Both the in-plane and perpendicular components of the strain, ε_{yy} and ε_{xx} respectively, show relaxation at the edge of the structure with the largest relaxation occurring close to, but not at, the edge. For the case of four strained layers, each layer has a strain distribution similar to that for the single layer, but, for layer-to-layer separations of 10.0 nm and 7.0 nm, the material between the layers becomes significantly strained near the edge of the sample. At a layer separation of 16.5 nm the strain distributions in each layer are nearly independent of their neighbours. If the elastic constants are assumed to be isotropic, the results differ only slightly (less than 6%) from those obtained from the full anisotropic calculation. For the isotropic case, the maximum shear strain for a strained layer of Poisson's ratio ν and mismatch f is found to be $0.68f(1 + \nu)/(1 - \nu)$. The minimum value of the strain relaxation perpendicular to the plane of the layer, ε_{xx}, is $f(0.10 - 0.82\nu)(1 + \nu)/(1 - \nu)$ while the maximum value of the in-plane strain relaxation, ε_{yy}, is $f(0.90 - 1.19\nu)(1 + \nu)/(1 - \nu)$.

1. Introduction

The ability to grow high-quality strained-layer semiconductor structures has led to a new class of electronic and optoelectronic devices (Osbourn 1982, O'Reilly 1989). The biaxial strain, which is usually accommodated elastically within the strained layer, modifies the band structure and hence the electronic properties of the device. Careful control of the composition (and therefore the strain) enables devices with appropriate electronic properties to be uniquely tailored. Although the strain in the bulk of a structure can be deduced from the composition of the materials (provided these are accurately known), its value at the edge of the structure can be quite different because the strain is able to

0953-8984/90/5110289 + 14 $03.50

relax at the free surface. It is the calculation of the stress/strain distribution at the edge of strained-layer structure that is the focus of the present paper.

There is ample evidence that strain relaxation occurs at the edge of structures containing strained layers (Auret *et al* 1979, Treacy *et al* 1985, Gibson *et al* 1985, Bangert *et al* 1989a, b). The bending of the diffraction contrast in transmission electron microscopy (TEM) provides a sensitive probe of the relaxation process. In fact, previous calculations have been geared towards the interests of electon microscopists because the thin samples required for their experiments make it necessary to have a detailed knowledge of the strain relaxation effects near free surfaces. Auret *et al* (1979), for example, combined a simple numerical strain calculation with the dynamical theory of strain contrast and obtained excellent agreement with experimental diffraction contrasts from their InGaAs/GaAs samples. They suggested that measurements of strain relaxation close to free surfaces could lead to accurate determination of the indium concentration in the strained layer. The calculations of Treacy and co-workers (Treacy *et al* 1985, Gibson *et al* 1985, Treacy and Gibson 1986) are particularly noteworthy and the theory presented in this paper expands on their work. They demonstrate that an analysis of strain relaxation in thin samples is essential to the interpretation of TEM images. More recently, results from TEM diffraction contrasts on wedge samples have been compared to 3D strain calculations obtained using finite-element techniques (Bangert *et al* 1989a, b). Again, good qualitative agreement between experiment and theory has been obtained.

There are additional reasons for which a knowledge of the strain distribution at the edge of strained structures is important. Both during the growth of the structure and during device fabrication the strained layers are exposed at free surfaces. Edge regions have been shown to be the source of dislocations in some device structures (Sim *et al* 1988). In the present paper it is demonstrated that the relaxation of the strained layer at a free surface introduces regions of shear strain which may be the source of these dislocations. Other questions also remain to be resolved. For instance, the extent to which one strained layer influences the strain distribution in a neighbouring layer is of technological importance and is addressed here for the first time.

We focus our attention on the mesa laser structure studied by Tothill *et al* (1990) although the results obtained are of general significance for a wide variety of strained-layer structures. The theory is presented in section 2 and the results, both for a single strained layer and for four strained layers, are presented in section 3. Finally, the conclusions may be found in section 4.

2. Theory

A typical mesa structure is shown in figure 1. The z dimension of the structure is large compared to either the x or the y dimension and so it is only necessary to examine the 2D slice as indicated in figure 1. The mesa structure examined by Tothill *et al* (1990) contains four strained layers of $In_{0.7}Ga_{0.3}As$ grown on InGaAsP (lattice matched to InP) with a fractional lattice mismatch f is 0.009. This structure is illustrated in the inset of figure 1. The 2D slice is shown in figure 2 and contains a single strained layer (rather than four as in the mesa structure) with the y axis in the plane of the layer and the x axis parallel to the growth direction. The important dimensions are a, the layer half-thickness, c, the half-thickness in the y direction and l, the half-thickness in the x direction. Occasionally it is convenient to refer to the full layer thickness w, where $w = 2a$.

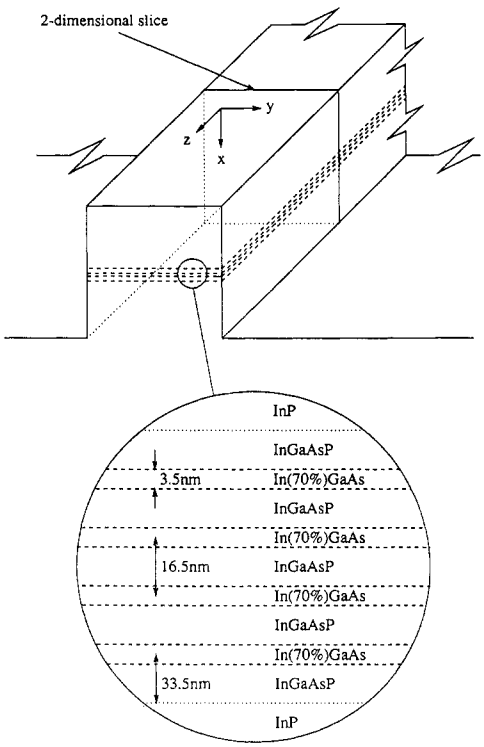

Figure 1. A schematic diagram of the mesa structure studied by Tothill *et al* (1990). Calculations are performed for the 2D slice indicated. The mesa structure consists of four strained layers of $In_{0.7}Ga_{0.3}As$ in InGaAsP barriers lattice matched to InP.

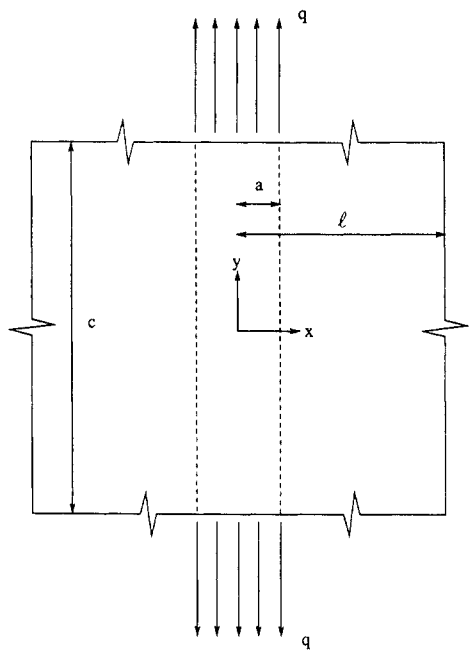

Figure 2. A schematic diagram of the 2D slice through the mesa structure. This section contains a single strained layer. The biaxial strain within the layer is equivalent to a stress of magnitude q acting in the y and z directions.

The analysis which follows assumes that the materials are continuous, deform elastically and that plane-strain conditions exist. The condition of plane strain is equivalent to an infinite thickness in the z direction. This is an appropriate approximation for the mesa structure where the z dimension is several orders of magnitude larger than the thicknesses $2c$ or $2l$. Plane-strain conditions ensure that all displacements are confined to the x–y plane with zero displacement in the z direction. The x, y and z axes are assumed to refer to the crystallographic [100], [010] and [001] directions respectively. For simplicity it is assumed that the elastic constants have the same values for both the layer and barrier materials (although this is not a restriction on the theory) and correspond to those for InAs. We also assume that strain relaxation due to the presence of dislocations is negligible (the layer is below its critical thickness) and that compositional (and hence strain) fluctuations may be neglected. Within the framework of these assumptions, expressions for the stress and strain components may be derived.

First, however, the value of the strain in the bulk of a strained layer, away from any free surface, is discussed. The strain at the centre of a strained layer in the in-plane (y and z) directions is simply equal to $-f$, where f is the fractional lattice mismatch between the layer and the barrier, and the negative sign indicates that the layer is under

compression. Perpendicular to the plane (in the x direction) the strain is easily shown via Hooke's laws to equal $2\nu f/(1-\nu)$, where the Poisson's ratio ν is the value for the [100] crystallographic directions and is equal to $c_{12}/(c_{11}+c_{12})$. For the case of InAs, the elastic constants are $c_{11} = 86.5$ GN m^{-2}, $c_{12} = 48.5$ GN m^{-2} and $c_{44} = 39.6$ GN m^{-2} (Reifenberger *et al* 1969).

The strain relaxation at free surfaces may now be calculated. The derivation outlined below is based on that presented by Timoshenko and Goodier (1970) and Treacy and Gibson (1986). 2D stress/strain problems require the determination of the Airy stress function φ, which satisfies the following relation,

$$\partial^4\varphi/\partial x^4 + B\,\partial^4\varphi/\partial x^2\,\partial y^2 + \partial^4\varphi/\partial y^4 = 0 \tag{1}$$

where the familiar stress components are related to φ by the simple relations

$$\sigma_{xx} = \partial^2\varphi/\partial y^2 \qquad \sigma_{yy} = \partial^2\varphi/\partial x^2 \qquad \sigma_{xy} = -\partial^2\varphi/\partial x\,\partial y. \tag{2}$$

The stresses σ_{xx}, σ_{yy} and σ_{xy} are the x component, y component and shear stress in the x–y plane respectively. In some texts the notation σ_x, σ_y and τ_{xy} are used for these components but as the following treatment follows that of Treacy and Gibson, we retain their notation. If the material is isotropic, the quantity B in equation (1) is equal to 2. B is related to the anisotropy coefficient A which is in turn related to the elastic constants of the material.

$$B = 2[A(c_{11}+2c_{12}) - c_{12}]/(c_{11}+c_{12}) \tag{3}$$

$$A = (c_{11}-c_{12})/2c_{44}. \tag{4}$$

A is equal to 1 for an isotropic material and for InAs the value of A is 0.48.

It is now necessary to determine φ for the single strained layer illustrated in figure 2. The elastic strain contained within the layer is equivalent to a stress of magnitude q acting perpendicular to the surface. The stress q, if applied as a compressive stress in the y and z directions to a relaxed isolated layer (no barriers), would introduce strains of $-f$ in the y and z directions and $2\nu f/(1-\nu)$ in the x direction. The applied stress q is therefore easily evaluated from Hooke's laws (see equation (14)) by placing ε_{yy} and ε_{zz} equal to f, σ_{yy} and σ_{zz} equal to q and σ_{xx} equal to 0. The final expression for q is

$$q = Ef/(1-\nu) \tag{5}$$

where E, the Young's modulus in the [100] direction, is equal to $(c_{11}-c_{12})(c_{11}+2c_{12})/(c_{11}+c_{12})$. In order to evaluate the stress components, we note that the stress σ_{yy} across the surface at $y = +c$ (or $y = -c$) has a constant value q when $-a < x < a$ and is zero otherwise. It is possible to represent this step function by a Fourier series and so a reasonable form for the Airy stress function is

$$\varphi = \sum_{m=0}^{\infty} A_m \cos(m\pi x/l) f_m(y) \tag{6}$$

where cosines are chosen because the load is symmetric about $x = 0$. This expression for φ is appropriate for problems with specified boundary conditions on the faces $y = \pm c$ but the choice of φ given in equation (6) cannot include boundary conditions which may need to be specified on the faces $x = \pm l$. This would pose a problem if l was of the order of a, but for the mesa structure under consideration here the value of l is much larger than a and this choice of φ is therefore appropriate.

The y dependence of φ is contained within the function $f_m(y)$ where the subscript indicates that the function also depends on the summation index m. This contribution has been determined by Treacy and Gibson (1986) and the full method of evaluation may be followed in their appendix A. The final expressions for σ_{xx}, σ_{yy} and σ_{xy} obtained here differ slightly due to the presence of the cosine Fourier series rather than the simple sine function used by Treacy and Gibson. Note also that there are two small errors in the appendix A of Treacy and Gibson. An i should precede the second term in the equation (A11) and a factor $(\alpha t/2)$ should be inserted in equation (A13c). The final expressions are

$$\sigma_{xx} = -2 \sum_{m=1}^{\infty} A_m \cos \alpha x[\beta c(C - D) - \gamma c(E + F)]/R \tag{7}$$

$$\sigma_{yy} = +2 \sum_{m=1}^{\infty} A_m \cos \alpha x[\beta c(C - D) + \gamma c(E + F)]/R - A_0 \tag{8}$$

$$\sigma_{xy} = -2 \sum_{m=1}^{\infty} A_m \sin \alpha x[\alpha c(G - H)]/R \tag{9}$$

$C = \cosh \beta c \sin \gamma c \cosh \beta y \cos \gamma y \quad F = \sinh \beta c \cos \gamma c \cosh \beta y \cos \gamma y$

$D = \sinh \beta c \cos \gamma c \sinh \beta y \sin \gamma y \quad G = \cosh \beta c \sin \gamma c \sinh \beta y \cos \gamma y$

$E = \cosh \beta c \sin \gamma c \sinh \beta y \sin \gamma y \quad H = \sinh \beta c \cos \gamma c \cosh \beta y \sin \gamma y$

$R = \beta c \sin 2\gamma c + \gamma c \sinh 2\beta c \quad \beta = \tfrac{1}{2}\alpha(2 + B)^{1/2}$

$\gamma = \tfrac{1}{2}\alpha(2 - B)^{1/2} \quad \alpha = m\pi/l$

and B has been defined earlier. The coefficients A_m are easily obtained from standard Fourier analysis and are

$$\begin{aligned} A_m &= 2q \sin \alpha a/\alpha l \qquad m \neq 0 \\ A_0 &= qa/l. \end{aligned} \tag{10}$$

The summations in equations (7)–(9) are now taken from $m = 1$ to ∞ with the $m = 0$ contribution treated separately. For σ_{xx} and σ_{xy} this contribution is zero, whilst for σ_{yy} this contribution is equal to $-qa/l$. Placing $y = \pm c$ in expressions (8) and (9) reduces σ_{yy} to the simple Fourier series expression for the step function, while σ_{xy} is equal to 0 as required by the boundary conditions on the upper and lower faces. For ease of computation, expressions (7)–(9) simplify greatly when αy (and hence also αc) is large (greater than about 10). The simplified expressions are

$$\sigma_{xx} = -\sum_{m=1}^{\infty} A_m \cos \alpha x \, e^{-\beta(c-y)}(\beta U/\gamma - V) \tag{11}$$

$$\sigma_{yy} = +\sum_{m=1}^{\infty} A_m \cos \alpha x \, e^{-\beta(c-y)}(\beta U/\gamma + V) - qa/l \tag{12}$$

$$\sigma_{xy} = -\sum_{m=1}^{\infty} A_m \sin \alpha x \, e^{-\beta(c-y)} \, \alpha U/\gamma \tag{13}$$

$U = \sin \gamma c \cos \gamma y - \cos \gamma c \sin \gamma y \quad V = \sin \gamma c \sin \gamma y + \cos \gamma c \cos \gamma y.$

The three stress components are calculated using equations (6)–(13) with equations (11)–(13) used for values of m for which αy is greater than 10.

The strain components are determined using the Hooke's law relations,

$$\varepsilon_{xx} = [\sigma_{xx} - \nu(\sigma_{yy} + \sigma_{zz})]/E \tag{14}$$

with two similar expressions involving ε_{yy} and ε_{zz}. These relations are used to obtain expressions for the strain components under plane-strain conditions. There is no strain relaxation in the z direction, as discussed earlier, and so ε_{zz} is set equal to 0. Eliminating σ_{zz} yields

$$\varepsilon_{xx} = [(1 - \nu^2)\sigma_{xx} - \nu(1 + \nu)\sigma_{yy}]/E \tag{15}$$

$$\varepsilon_{yy} = [(1 - \nu^2)\sigma_{yy} - \nu(1 + \nu)\sigma_{xx}]/E. \tag{16}$$

Finally, it is noted that the shear strain ε_{xy} is related directly to σ_{xy} by

$$\varepsilon_{xy} = 2(1 + \nu)\sigma_{xy}/E. \tag{17}$$

It is important to appreciate that equations (15)–(17) determine the *strain relaxation*. If two points within the material (arbitrarily close) do not move relative to each other under the action of the stress q, then the calculated value of the strain relaxation is equal to zero. A positive value of the strain relaxation indicates an expansion of the material and a negative value indicates contraction of the material relative to the starting configuration illustrated in figure 2. If, for instance, the calculation leads to a value $+f$ of ε_{yy} at some point in the layer, the layer has expanded by a fraction f in the in-plane direction at this specific point and has thus relaxed back to its preferred atomic spacing. The true strain in the material may be obtained by adding the initial conditions: that is by adding $-f$ to the calculated values of ε_{yy} in the layer and by adding $2\nu f/(1 - \nu)$ to the calculated values of ε_{xx}, also within the layer. Of course, in the barrier, the initial conditions are of zero strain and so the calculated strain relaxation using equations (15)–(17) is equal to the true strain. We discuss the results in terms of strain relaxation in the following section and make reference to the true strain as appropriate. We also note that, if the barriers are removed from figure 2 to leave the isolated layer, the applied stress q would introduce an in-plane strain ε_{yy} of $f(1 + \nu)$ and not f. This is because the layer is still subject to plane strain conditions and therefore cannot relax in the z direction.

The equations produced so far include anisotropic effects through the parameter B which is related to the anisotropy coefficient A (equations (3) and (4)). Many semiconductor materials have an anisotropy coefficient approximately equal to 0.5 indicating, for instance, that the Young's Modulus E is roughly twice as large in the [111] direction as it is in the [100] direction. Despite the large variation in E, it will be shown in section 3 that the results are not very sensitive to this anisotropy. Expressions for the strain components may be obtained for the isotropic case by setting B equal to 2, and therefore $\gamma = 0$ and $\beta = \alpha$. Equations (7)–(9) reduce to,

$$\sigma_{xx} = -2 \sum_{m=1}^{\infty} A_m \cos \alpha x[C' - D' - F']/R' \tag{18}$$

$$\sigma_{yy} = +2 \sum_{m=1}^{\infty} A_m \cos \alpha x[C' - D' + F']/R' - A_0 \tag{19}$$

$$\sigma_{xy} = -2 \sum_{m=1}^{\infty} A_m \sin \alpha x[G' - H']/R' \tag{20}$$

$$C' = \alpha c \cosh \alpha c \cosh \alpha y \qquad G' = \alpha c \cosh \alpha c \sinh \alpha y$$

$$D' = \alpha y \sinh \alpha c \sinh \alpha y \qquad H' = \alpha y \sinh \alpha c \cosh \alpha y$$

$$F' = \sinh \alpha c \cosh \alpha y \qquad R' = 2\alpha c + \sinh 2\alpha c.$$

Reduced expressions similar to (11)–(13) for large values of m may easily be determined from the above equations.

Using the procedure described above, a value of the stress at any point due to the presence of a single strained layer may be calculated. In order to evaluate the total stress at a point due to an arbitrary number of strained layers, we invoke the principle of superposition. This principle states that, provided that the displacements do not significantly affect the action of any forces, the total stress at a point is simply the sum of the individual stresses. Thus, within the framework of this assumption, we are able to estimate the stress/strain distribution due to an arbitrary number of strained layers by simply summing the stresses at a point which arise due to each layer.

3. Results

All results are obtained with $c_{11} = 86.5\ \mathrm{GN\,m^{-2}}$, $c_{12} = 48.5\ \mathrm{GN\,m^{-2}}$ and $c_{44} = 39.6\ \mathrm{GN\,m^{-2}}$ which leads to a value of the Young's modulus of $51.7\ \mathrm{GN\,m^{-2}}$ and a Poisson's ratio ν of 0.36 for the [100] crystallographic directions. These are the values for InAs (Reifenberger *et al* 1969). The values of c and l are fixed at 0.5 μm. The results are not sensitive to the values of c and l as both parameters are much larger than the layer width. The layer half-width a is equal to 1.75 nm and the mismatch f is 0.009. These values correspond to those of Tothill *et al* (1990). Calculations are performed using equations (6)–(13), (15)–(17) and include anisotropic effects in full. The results for the single strained layer and for the combination of four strained layers are considered separately in the following subsections.

3.1. The single strained layer

The shear strain distribution ε_{xy} is presented as a contour plot in figure 3. It is seen that the maximum shear strain occurs at the layer–barrier boundary close to the surface. Dislocations can form as a consequence of shear forces in the material which encourage atomic layers to slide over each other. These results therefore suggest that the most likely position for dislocations to form is in the region at the layer/barrier interface close to the surface of the structure. The maximum value of the shear strain is 1.3% in the present system. If the critical shear strain for this material is assumed to be about 5%, this value would be exceeded at the edge of the structure at mismatches of about 3.5% and above.

The shearing action can be seen in figure 4 which illustrates the displacement of the material near the free surface. Note that the squares represent a region of material that has become distorted due to strain relaxation at the edge of the structure and do not represent atomic spacings. The most distorted (or 'diamond-like') portion is at the layer–barrier boundary near the edge.

The strain components ε_{xx} and ε_{yy} are presented in contour plots in figures 5 and 6. Recall that a positive value of ε indicates that the material has stretched while a negative value indicates compression. In figure 5, ε_{xx} reaches a minimum in the centre of the well

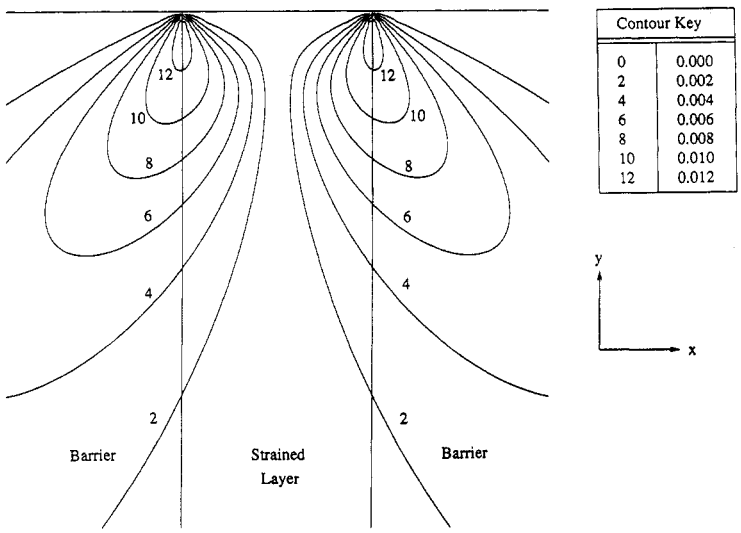

Figure 3. The shear strain ε_{xy} for a single strained layer of width 3.5 nm. The diagram covers a region 10 nm × 10 nm. The contours indicate curves of constant strain and are labelled in units of 10^{-3} as shown in the contour key.

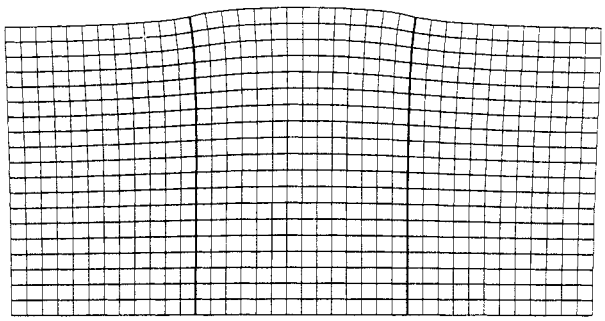

Figure 4. The displacements of the material close to the edge of the structure (exaggerated by a factor of 20). The figure shows the distortion of squares of material due to surface relaxation effects.

approximately 1.5–3 nm from the surface. This is the region where the atomic spacing in the x direction is closest to its relaxed value. There is, however, a region very close to the surface where ε_{xx} is positive, indicating that the material has stretched and therefore distorted even further from its relaxed atomic spacing. The 'bulging out' of the layer at the surface causes stretching in the x direction and hence an increase in ε_{xx}. The Poisson's ratio effect leads to a corresponding slight reduction in the value of ε_{yy} close to the surface which can be seen in figure 6. The maximum in-plane strain ε_{yy} is observed in the centre of the layer at approximately 1.2 nm from the surface. This strain is positive, of course, indicating that the layer has expanded close to the surface. Note also that there are small lobes of compression in the barrier material close to the edge of the structure which form in response to the bulging of the layer.

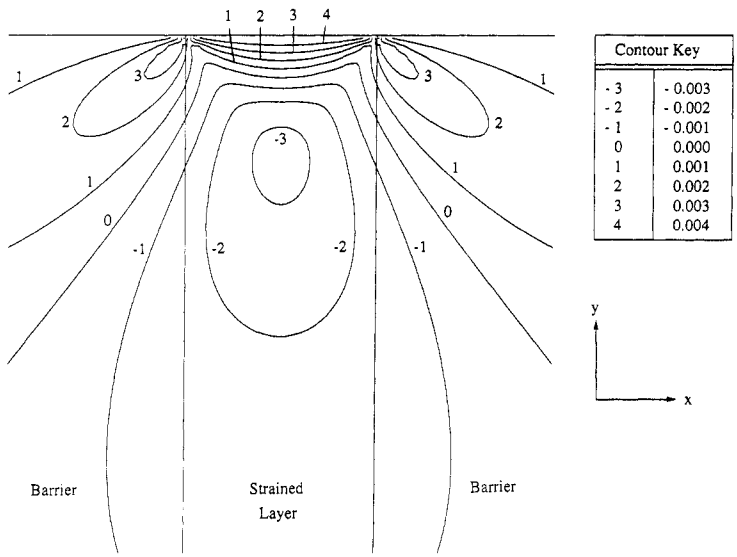

Figure 5. The strain component ε_{xx} for a single strained layer of width 3.5 nm. The diagram covers a region 10 nm × 10 nm. The contours indicate lines of constant strain and are labelled in units of 10^{-3} as shown in the contour key.

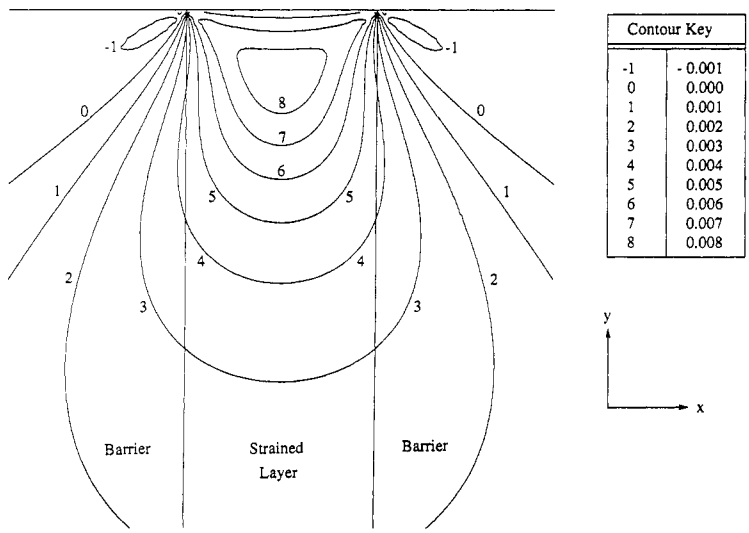

Figure 6. The strain component ε_{yy} for a single strained layer of width 3.5 nm. The diagram covers a region 10 nm × 10 nm. The contours indicate lines of constant strain and are labelled in units of 10^{-3} as shown in the contour key.

It is interesting to examine ε_{yy} in more detail. Figure 7 shows the value of ε_{yy} at the centre of the layer plotted as a function of the distance from the edge of the structure. It is clear that the most significant strain relaxation occurs from 0 to about 10 nm into the layer. Thereafter the decay is slow such that the value of ε_{yy} is equal to 10% and

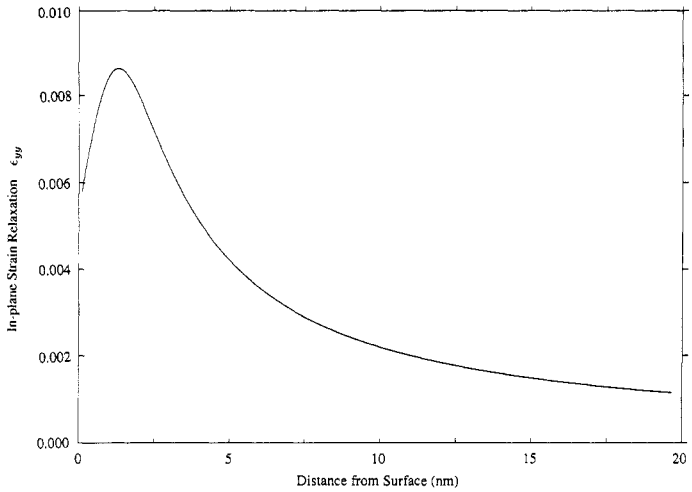

Figure 7. The strain component ε_{yy} at the centre of the layer plotted as a function of the distance from the free surface.

5% of f at distances of approximately 30 nm and 65 nm respectively. This means, for example, that the absolute value of the *true* strain in the strained layer (obtained, we recall, by adding the initial strain $-f$ to the calculated value) at a distance of 30 nm from the surface is $0.9f$, and at 65 nm from the surface the true strain is about $0.95f$. For a layer of arbitrary width w these calculations show that the majority of the strain relaxation occurs over a distance of roughly $3w$ into the material. The strain is $0.9f$ and $0.95f$ at distances of about $9w$ and $18w$ respectively.

It is clear from the previous discussion that only for very small samples would the average in-plane strain in the sample be significantly different from the mismatch f. This can be tested by evaluating the strain relaxation ε_{yy} at the centre of the structure for different values of c. It is found, for instance, that a sample with $c = 1$ μm possesses an average strain which differs from f by only 2.4% and a $c = 10$ μm sample differs by about 1.3%.

The influence of the anisotropy of the elastic constants on the strain relaxation may be assessed by evaluating the same quantities by using isotropic elastic constants. This involves setting $B = 2$ and fixing E and ν to the values for the [100] crystallographic directions. The stress components are evaluated using equations (18)–(20) and the strain relaxation components using equations (15)–(17). There is little difference between the results for the isotropic case and those for the case in which the anisotropy of elastic constants is fully included. The values of ε_{yy}, for instance, differ by at most 6%.

For the isotropic case, expressions for the maximum and minimum values of the strain relaxation components may be obtained for any strained layer. The maximum shear strain is found to be $\varepsilon_{xy,\max} = 0.68f(1 + \nu)/(1 - \nu)$. The in-plane strain relaxation, ε_{yy}, has a maximum value close to the edge of the structure of $\varepsilon_{yy,\max} = f(0.90 - 1.19\nu)(1 + \nu)/(1 - \nu)$ and the perpendicular component of the strain has a minimum value of $\varepsilon_{xx,\min} = f(0.10 - 0.82\nu)(1 + \nu)/(1 - \nu)$. If it is assumed that

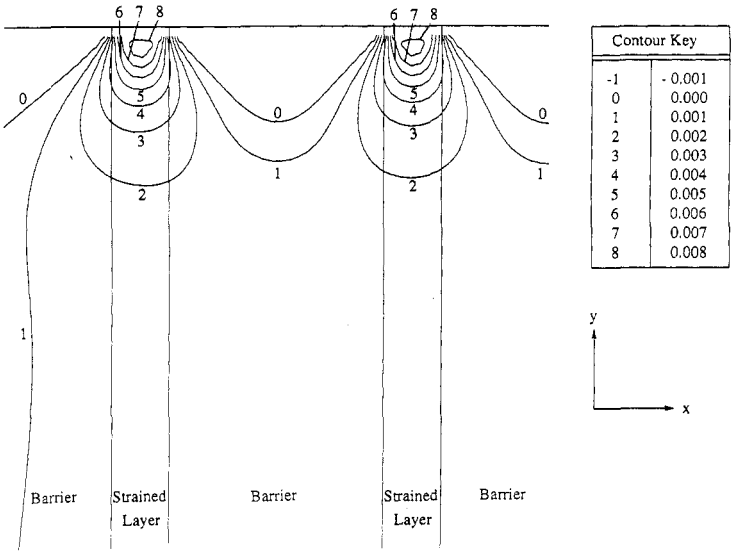

Figure 8. The strain ε_{yy} for four strained layers of width 3.5 nm separated by centre-to-centre distances of 16.5 nm. Only layers 1 and 2 are shown in the figure. The diagram covers a region 33 nm × 33 nm. The contours indicate lines of constant strain and are labelled in units of 10^{-3} as shown in the contour key.

Poisson's ratio ν is equal to $\frac{1}{3}$, these reduce further to $\varepsilon_{xy,\max} \simeq 1.36f$, $\varepsilon_{xx,\min} \simeq -0.35f$ and $\varepsilon_{yy,\max} \simeq f$ respectively.

3.2. *Four strained layers*

The principle of superposition, as explained in section 2, permits the calculation of the stress/strain distributions for the case of four strained layers. Each of the four layers has a half-width, a, of 1.75 nm and the centres of the layers are separated by a distance d. We concentrate on the results for the in-plane strain ε_{yy}.

The results for the structure examined by Tothill *et al* (1990), where $d = 16.5$ nm, are presented in figure 8. Layers 1 and 2 of the four strained layers are shown in the plot—layers 3 and 4 have distribution which are simply mirror images of those shown in the figure. Figure 8 shows that there is virtually no transmission of strain from one layer to another and that each behaves essentially as a single strained layer independent of the others. For comparison, results for $d = 10.0$ nm and $d = 7.5$ nm were also produced and these are shown in figures 9 and 10 respectively. In both cases significant transmission of strain into the barrier material between the layers is observed. When $d = 10.0$ nm, the maximum strain in the barrier is about 0.003, or about one third the misfit strain in the layer. The strain distribution in the layer itself, although somewhat asymmetric, is not substantially different from that in figure 8. For $d = 7.5$ nm, where the barrier material is the same thickness as the well, the strain in the barrier is in excess of 0.004. Thus, significant strain transmission is observed between layers if $d \leqslant 3w$. The magnitude of the shear strain at the maximum in each of the above cases does not alter significantly (although the distribution changes slightly away from the maximum) and so it may be

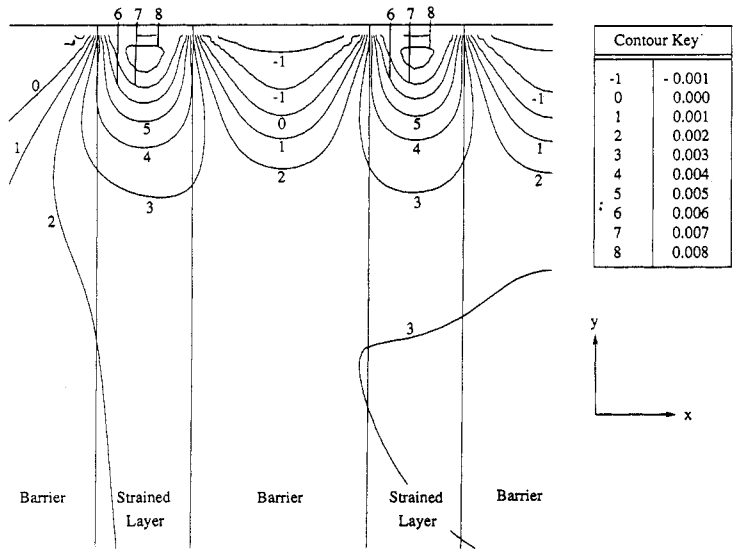

Figure 9. The strain ε_{yy} for four strained layers of width 3.5 nm separated by centre-to-centre distances of 10.0 nm. Only layers 1 and 2 are shown in the figure. The diagram covers a region 20 nm × 20 nm. The contours indicate lines of constant strain and are labelled in units of 10^{-3} as shown in the contour key.

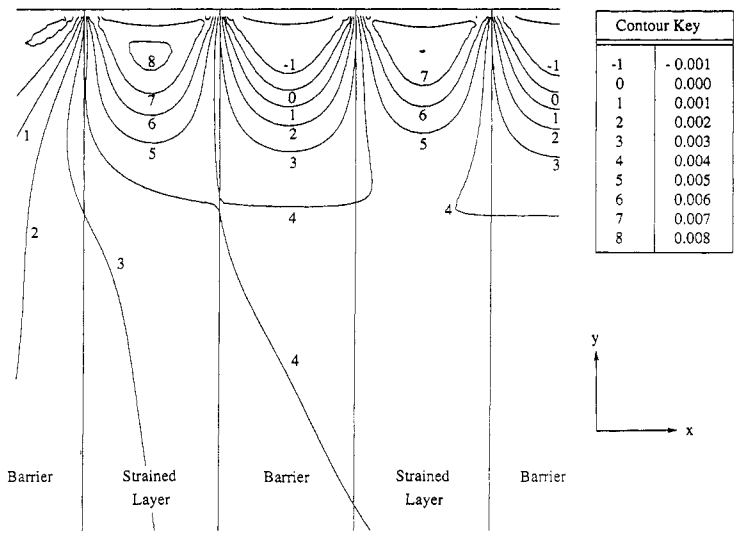

Figure 10. The strain ε_{yy} for four strained layers of width 3.5 nm separated by centre-to-centre distances of 7.0 nm. Only layers 1 and 2 are shown in the figure. The diagram covers a region 14 nm × 14 nm. The contours indicate lines of constant strain and are labelled in units of 10^{-3} as shown in the contour key.

concluded that the likelihood of dislocations forming at the surface due to shear strains is not significantly enhanced by the presence of four wells.

4. Conclusions

Calculations of strain distributions in strained-layer structures have been presented. The calculations are currently confined to two dimensions and we make the assumptions outlined in section 2. The conclusions from the investigations may be summarised as follows:

(i) The maximum shear strain is at the layer–barrier interface close to the edge of the structure. Dislocations arising due to the presence of shear strains are most likely to nucleate at these points. The maximum shear strain is approximately 1.3% for the mesa structure.

(ii) The results for ε_{xx} and ε_{yy} indicate that the strained layer relaxes at the edge of the structure, with the greatest relaxation in a region close to, but not at, the edge. In terms of the layer width w, the minimum value of ε_{xx} occurs at about $0.75\,w$ from the surface and the maximum value of ε_{yy} occurs at about $w/3$ from the surface.

(iii) The in-plane strain relaxation ε_{yy} in the layer occurs over a distance of about $3w$ from the free surface. The true in-plane strain in the layer is $0.9f$ and $0.95f$ at distances of about $9w$ and $18w$ from the edge, respectively.

(iv) Strain is significantly transferred to the barrier material near the edge of the structure if layers are separated by (centre-to-centre) distances of less than about $6w$. The four-layer structure with the layers separated by a distance of 16.5 nm showed little strain in the barriers and so the layers were not significantly influenced by their neighbours.

(v) The maximum value of the shear strain did not change significantly with the presence of neighbouring strained layers. Thus dislocations which nucleate as a consequence of shear strains are not significantly more likely to form in multilayer structures than in single strained-layer devices.

(vi) If it is assumed that the elastic constants are isotropic, expressions for the maximum and minimum strain relaxations may be obtained. The maximum shear strain is found to be $\varepsilon_{xy,\max} = 0.68f(1+\nu)/(1-\nu)$ while the in-plane strain relaxation has a maximum value close to the edge of the structure of $\varepsilon_{yy,\max} = f(0.90 - 1.19\nu)(1+\nu)/(1-\nu)$ and the perpendicular component of the strain has a minimum value of $\varepsilon_{xx,\min} = f(0.10 - 0.82\nu)(1+\nu)/(1-\nu)$.

Finally it is noted that this type of calculation is extremely flexible within the framework of the assumptions outlined in section 2. For instance, it is possible to study the strain relaxation in a strained layer which has a thin capping layer of barrier material or, alternatively, a surface strained layer such as an oxide coating. The flexibility of the Fourier series treatment would also allow the investigation of a layer with arbitrary compositional (and hence strain) variation. In all cases, results may be obtained for an arbitrary number of layers according to the principle of superposition. The results are likely to be unreliable, however, for thin structures containing only a few atomic layers as the continuum approximation will be least accurate in this regime.

Acknowledgment

One of us (DAF) would like to acknowledge the support of British Telecom Research Laboratories via the award of a short-term fellowship which enabled this work to be undertaken.

References

Auret P D, Ball C A B and Snyman H C 1979 *Thin Solid Films* **61** 289–95

Bangert U, Charsley P, Faux D A, Harvey A J, Dixon R, Goodhew P J, Emery M C and Whitehouse C R 1989a *Proc. Microscopy of Semiconducting Materials (VI, Oxford, 1989)* ed A G Cullis and J L Hutchinson (Bristol: Institute of Physics) pp 287–91

Bangert U, Harvey A J, Faux D A, Charsley P and Goodhew P J 1989b *EMAG/MICRO Proc. (London, 1989)* vol 1 (Bristol: Institute of Physics) pp 423–6

Gibson J M, Hull R and Bean J C 1985 *Appl. Phys. Lett.* **46** 649–51

O'Reilly E P 1989 *Semicond. Sci. Technol.* **4** 121–37

Osbourn G C 1982 *J. Appl. Phys.* **53** 1586–9

Reifenberger R, Keck M J and Trivisonno J 1969 *J. Appl. Phys.* **40** 5403–4

Sim S P, Skeats A P, Taylor M R, Hockley M, Cooper D M, Nelson A W, Devlin W J and Regnault J C 1988 *Proc. 14th European Conf. on Optical Commun. (ECOC88) (Brighton, 1988)* part 1 (London: IEE) pp 396–9

Timoshenko S P and Goodier J N 1970 *Theory of Elasticity* (New York: McGraw-Hill) ch 3

Tothill J N, Wilkie J H, Westbrook L, Hatch C B, Halliwell M A G and Lyons M H 1990 *J. Electron. Mater.* in preparation

Treacy M M J and Gibson J M 1986 *J. Vac. Sci. Technol.* B **4** 1458–66

Treacy M M J, Gibson J M and Howie A 1985 *Phil. Mag.* **51** 389–417